molecules

MDPI

*Review*

# Functionalization of Endohedral Metallofullerenes with Reactive Silicon and Germanium Compounds †

**Masahiro Kako [1,*], Shigeru Nagase [2,*] and Takeshi Akasaka [3,4,5,6,*]**

1 Department of Engineering Science, The University of Electro-Communications, Chofu 182-8585, Japan
2 Fukui Institute for Fundamental Chemistry, Kyoto University, Kyoto 606-8103, Japan
3 Life Science Center of Tsukuba Advanced Research Alliance, University of Tsukuba, Ibaraki 305-8577, Japan
4 Department of Chemistry, Tokyo Gakugei University, Tokyo 184-8501, Japan
5 Foundation for Advancement of International Science, Ibaraki 305-0821, Japan
6 School of Materials Science and Engineering, Huazhong University of Science and Technology, Wuhan 430074, China
* Correspondence: kako@e-one.uec.ac.jp (M.K.); nagase@ims.ac.jp (S.N.); akasaka@tara.tsukuba.ac.jp (T.A.); Tel.: +81-42-443-5570 (M.K.)
† Dedicated to Professor Marian Mikołajczyk on the occasion of his 80th birthday.

Academic Editor: Kyriakos Porfyrakis
Received: 20 May 2017; Accepted: 10 July 2017; Published: 14 July 2017

**Abstract:** Exohedral derivatization of endohedral metallofullerenes (EMFs) has been exploited as a useful method for characterizing the structural and chemical properties of EMFs, and for functionalizing them for potential applications. The introduction of heteroatoms, such as electropositive silicon atoms, to fullerene cages is a novel functionalization method that remarkably affects the electronic characteristics of fullerenes. This review comprehensively describes the results of the reactions of monometallofullerene, dimetallofullerene, and trimetallic nitride template EMFs with disilirane, silirane, silylene, and digermirane, which afforded the corresponding silylated and germylated fullerenes. Several examples emphasize that exohedral functionalization regulates the dynamic behaviors of the encapsulated metal atoms and clusters in the fullerene cages. The electronic effects of silyl and germyl groups are represented by comparing the redox properties of silylated and germylated EMFs with those of other EMFs derivatized with carbon-atom-based functional groups.

**Keywords:** endohedral metallofullerene; silylation; germylation; disilirane; silirane; silylene; digermirane

## 1. Introduction

Endohedral metallofullerenes (EMFs) are attracting great interest because of their unique structures and properties [1–15]. Encapsulation of metal atoms and metal clusters inside EMFs results in electron transfer from the inner species to the carbon cages. Results of earlier studies show that EMFs have remarkable electronic properties such as oxidation and reduction potentials. The difference in redox potentials between EMFs and hollow fullerenes is a key factor characterizing the properties and reactivities of EMFs.

Exohedral derivatization of EMFs and empty fullerenes has been explored extensively as an effective method to modify and enhance the characteristics of fullerenes for various nanomaterials science and biomedicine applications [1–15]. To date, many reactions have been applied for the exohedral derivatization of EMFs with respect to their use for functional materials. However, the derivatization reactions of EMFs remain sparse compared to those of empty fullerenes. In many cases, the derivatizing organic groups are bonded covalently to the carbon cages of EMFs through C–C

bonds. Therefore, derivatization that exploits the heteroatom properties is expected to contribute to the development of EMFs as functional materials.

In this context, derivatization of fullerenes using silicon and germanium atoms is an attractive method for modifying the electronic properties of fullerenes because of the electron-donating effects of silyl and germyl groups [16–19]. We found that the reactions of empty fullerenes with reactive silicon and germanium compounds afforded the corresponding fullerene derivatives [20–32]. These results prompted us to investigate properties of EMFs by examining their reactivities toward silicon and germanium compounds. The combination of fullerenes and silicon and germanium compounds provide a basis for the production of novel functional materials for electronic device, as mentioned in the section on potential applications. This review presents a summary of our results of silylation and germylation reactions as part of our continuing investigation of the chemical functionalization of EMFs [1,4–8,11,12,15]. We demonstrate that the introduction of silicon and germanium atoms markedly perturbs the electronic properties of fullerenes because of the electron-donating effects of these atoms. More specifically, derivatization of EMFs using reactive compounds containing heavier group 14 elements, such as silylene (silicon analog of carbene), disilirane (disilacyclopropane), silirane (silacyclopropane), and digermirane (digermacyclopropane) will be outlined. For several silylated and germylated derivatives of EMFs, the electronic properties are discussed in comparison with reference compounds that possess the same addition patterns because the redox behaviors of derivatized EMFs depend on the regiochemistry of the addends on the carbon cages. We also describe how derivatization with organosilicon compounds influences the behaviors of encapsulated metal atoms. In this review, we will focus on the functionalization of the following EMFs: La@$C_{2v}$-$C_{82}$, $La_2$@$I_h$-$C_{80}$, $Ce_2$@$I_h$-$C_{80}$, $Ce_2$@$D_{3h}$-$C_{78}$, $Sc_3N$@$I_h$-$C_{80}$, and $Lu_3N$@$I_h$-$C_{80}$ (Figure 1).

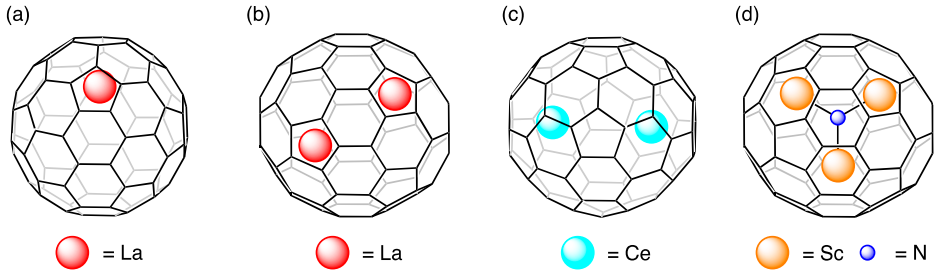


**Figure 1.** Structures of (**a**) La@$C_{2v}$-$C_{82}$; (**b**) $La_2$@$I_h$-$C_{80}$; (**c**) $Ce_2$@$D_{3h}$-$C_{78}$; and (**d**) $Sc_3N$@$I_h$-$C_{80}$.

## 2. Comparative Studies of Reactions of EMFs with Disilirane

In 1995, the first chemical derivatization of EMFs was achieved by the photochemical reaction of La@$C_{2v}$-$C_{82}$ and disilirane **1** [33]. It is particularly interesting that La@$C_{2v}$-$C_{82}$ reacted both thermally and photochemically with **1** to afford the corresponding adduct, although the empty fullerenes $C_{60}$ and $C_{70}$ did not react with **1** under thermal reactions in the absence of photoirradiation [21,23]. This result can be reasonably explained by the higher electron-accepting ability of La@$C_{2v}$-$C_{82}$ than that of empty fullerenes. Since this discovery, the reactivities of various EMFs have been investigated using **1** as a chemical probe (Scheme 1). Digermirane **3** reacted with La@$C_{2v}$-$C_{82}$ showing higher thermal reactivity than **1**, which results from the enhanced electron-donating property of **3** [34].

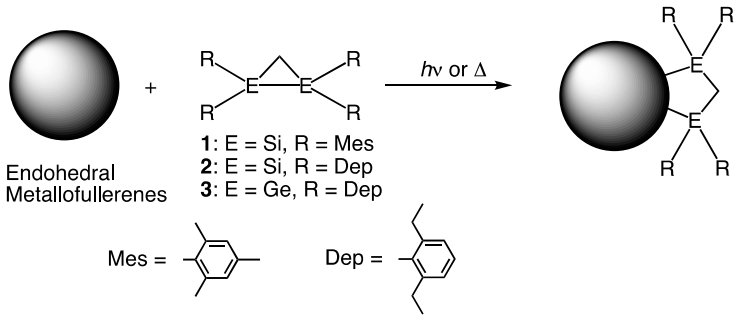


**Scheme 1.** Synthesis of disilirane and digermirane adducts of EMFs.

Redox potentials of selected EMFs and empty fullerenes are shown in Figure 2. Values of the first reduction (denoted as $E^{red}{}_1$) potentials are regarded as an important index for the reactivities toward **1** because fullerenes are believed to function as electron acceptors toward **1**, which is a good electron donor [15]. All the fullerenes shown in Figure 2 reacted with **1** by photoirradiation to afford the corresponding adducts. However, the EMFs and empty fullerenes with lower $E^{red}{}_1$ potentials did not undergo addition reactions under thermal conditions at 80 °C [15]. For example, $La_2@I_h$-$C_{80}$ reacted with **1** both photochemically and thermally [35], although $Sc_3N@I_h$-$C_{80}$ was found to be reactive only under photolytic conditions [36,37], although the first oxidation (denoted as $E^{ox}{}_1$) potentials of these EMFs are similar. Therefore, the higher thermal reactivity of $La_2@I_h$-$C_{80}$ toward **1** might be attributed to its good electron acceptor properties.

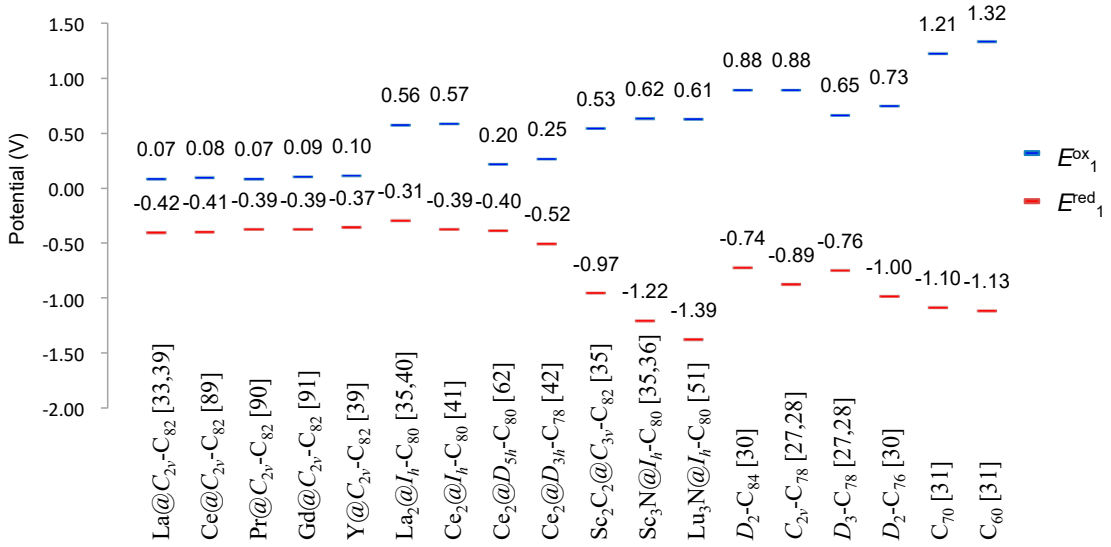


**Figure 2.** Redox potentials of EMFs and empty fullerenes. Values are in V relative to the ferrocene/ferrocenium couple ($Fc/Fc^+$).

It is noteworthy that the reactivities of EMFs were tunable by chemical oxidation or reduction [38]. Oxidation of La@$C_{2v}$-$C_{82}$ by $(p\text{-}BrC_6H_4)_3N^+SbCl_6^-$ produced the corresponding cation, $[La@C_{2v}\text{-}C_{82}]^+SbCl_6^-$, which reacted with **1** even at room temperature. In contrast, the addition of $NaSCH_3$ to La@$C_{2v}$-$C_{82}$ afforded the corresponding anionic species, $Na^+[La@C_{2v}\text{-}C_{82}]^-$, which was found to be inert to **1**. These results demonstrate that the electrophilicity of EMFs plays an important role in controlling their reactivities toward **1**.

## 3. Reactions of La@$C_{2v}$-$C_{82}$ with Disilirane 1

Figure 2 shows that La@$C_{2v}$-$C_{82}$ is highly reactive toward **1** because of its good electron-accepting ability. The molecular symmetry of La@$C_{2v}$-$C_{82}$, which possesses 24 non-equivalent carbon atoms in the $C_{2v}$-$C_{82}$ cage, is low. Therefore, addition reactions of La@$C_{2v}$-$C_{82}$ might produce multiple structural isomers. In fact, thermal reactions of La@$C_{2v}$-$C_{82}$ with **1** afforded at least six isomers of the mono-adducts based on analysis of the EPR spectrum of the reaction mixture [33]. A similar result was obtained for the thermal addition of digermirane **3** [34], indicating that the addition reactions of **1** and **3** to La@$C_{2v}$-$C_{82}$ were not regioselective.

The major isomer of the adducts derived from the reaction of La@$C_{2v}$-$C_{82}$ with **1** was isolated using HPLC separation [39]. The EPR spectrum of this isomer showed only one set of an octet hyperfine that was smaller than that of pristine La@$C_{2v}$-$C_{82}$. The addition of **1** also caused a change in the absorption spectrum, suggesting that the $\pi$-conjugation of the carbon cage was altered. Although the structures of the disilirane adducts of La@$C_{2v}$-$C_{82}$ have not been determined, their redox properties were obtained from electrochemical measurements. The results show that the $E^{\circ x}{}_1$ and $E^{red}{}_1$ potentials of the disilirane adducts of La@$C_{2v}$-$C_{82}$ were shifted cathodically, respectively, by 140 mV and 80 mV. These cathodic shifts of the redox potentials of silylated derivatives of EMFs are reasonably explained by the electron-donating effects of the silyl group, including $\sigma$–$\pi$ conjugation between the C–Si $\sigma$-orbitals and the $\pi$-orbitals of the fullerene cages [16–19]. The reaction of Y@$C_{2v}$-$C_{82}$ with **1** afforded two isomeric products as the 1:1 adducts, for which the cathodic shifts of redox potentials were observed compared to those of pristine Y@$C_{2v}$-$C_{82}$ [39].

## 4. Reactions of $La_2$@$I_h$-$C_{80}$ and Related EMFs with Disiliranes 1 and 2

Due to the symmetrical structure of the $I_h$-$C_{80}$ cage, the number of isomers is limited in the addition reactions of $La_2$@$I_h$-$C_{80}$. Only two non-equivalent carbon atoms exist in the $I_h$-$C_{80}$ cage: one is shared by one five-membered ring and two six-membered rings (denoted as the [5,6,6]-ring junction); the other is shared by three six-membered rings (denoted as the [6,6,6]-ring junction). The $I_h$-$C_{80}$ cage also has two non-equivalent C–C bonds: one is shared by one five-membered ring and one six-membered ring (denoted as the [5,6]-ring junction); the other is shared by two six-membered rings (denoted as the [6,6]-ring junction).

Heating a toluene solution of $La_2$@$I_h$-$C_{80}$ and disilirane **2** at 80 °C afforded the corresponding 1:1 adduct **5** as the sole product [40] (Scheme 2). The NMR and X-ray crystallographic analyses established the structures of **5** as the 1,4-adduct, indicating that the silyl groups are bonded to the [5,6,6]-junctions of the $I_h$-$C_{80}$ cage. In the crystal structure, the two encapsulated metal atoms were located close to the two six-membered rings on the equator of the cage. The reaction of $La_2$@$I_h$-$C_{80}$ and **1** produced a similar adduct **4**. The corresponding adduct of $Ce_2$@$I_h$-$C_{80}$ **6** was also obtained by a similar thermal reaction with **1**, showing the same 1,4-addition pattern [41] (Scheme 2).

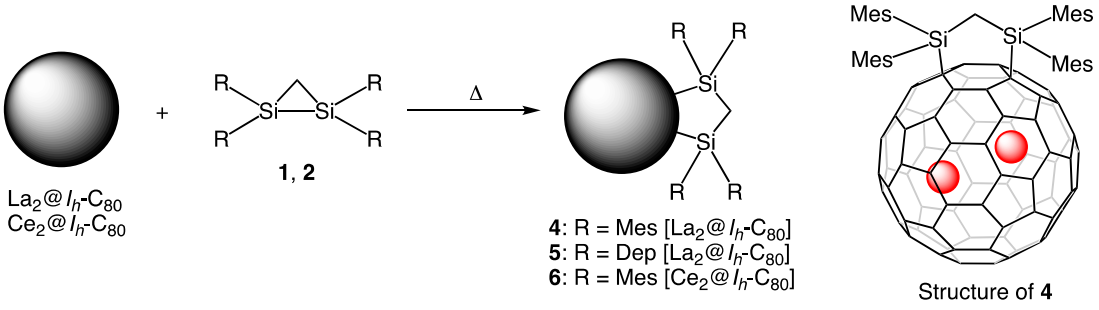


**Scheme 2.** Synthesis of disilirane adducts of $M_2$@$I_h$-$C_{80}$ (M = La, Ce).

In this review, the parent EMFs are shown respectively in brackets.

Scheme 3 shows that $Ce_2@D_{3h}$-$C_{78}$ also reacts readily with disilirane **1** to produce the corresponding 1,4-adduct **7** [42]. Based on X-ray crystallographic studies, the Ce atoms were found to be located at two positions facing the six-membered rings on the $C_3$ axis of the $D_{3h}$-$C_{78}$ cage. In the paramagnetic $^{13}$C-NMR spectral analysis, the observed carbon signals were more temperature-dependent than those of pristine $Ce_2@D_{3h}$-$C_{78}$. Therefore, the two Ce atoms in **7** likely interact with the $C_{78}$ cage more firmly than those in pristine $Ce_2@D_{3h}$-$C_{78}$ [42].

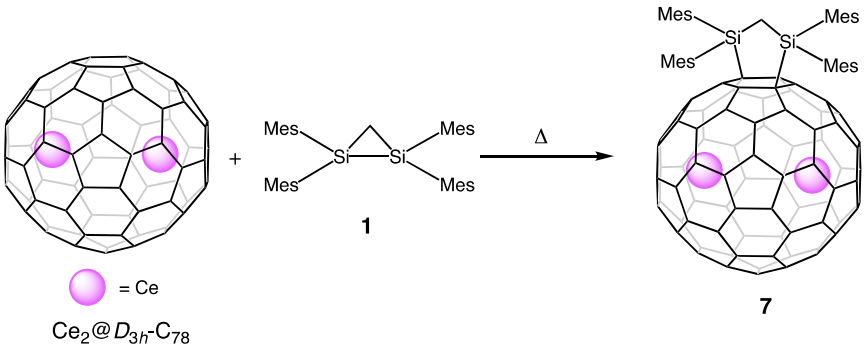


**Scheme 3.** Synthesis of a disilirane adduct of $Ce_2@D_{3h}$-$C_{78}$.

## 5. Reactions of $La_2@I_h$-$C_{80}$ with Silirane 8

Scheme 4 shows that $La_2@I_h$-$C_{80}$ also reacts with silirane **8** under thermal conditions to afford the corresponding 1,2-carbosilylated derivatives **9a** and **9b** [43]. Structural analyses, including X-ray crystallographic measurements, determined **9a** and **9b** to be a pair of diastereomers of the [5,6]-adducts. Furthermore, electrochemical measurements revealed that carbosilylation slightly altered the electronic properties of $La_2@I_h$-$C_{80}$. Results of X-ray crystallographic analysis showed that the crystal structure of **9a** has eight sites for the La atoms because of disorder [43]. Theoretical calculations of adducts of $La_2@I_h$-$C_{80}$ and **8** indicated that changing the La atom positions resulted in the differences in relative energies within the range of 0.85–5.89 kcal mol$^{-1}$. These small energy differences suggest the movability of the La atoms inside the cage [43]. The La atoms sites are arranged along the ten contiguously fused six-membered rings that constitute part of the $I_h$-$C_{80}$ cage.

Figure 3 presents the redox potentials of pristine and derivatized dimetallofullerenes. Remarkable cathodic shifts of both the $E^{ox}{}_1$ and $E^{red}{}_1$ potentials were observed for the silylated derivatives **4**, **5**, **9a** and **9b** relative to that of pristine $La_2@I_h$-$C_{80}$. Results also confirmed that the redox potentials shifted cathodically as the number of silicon atoms introduced into $La_2@I_h$-$C_{80}$ increased as shown by those of **4**, **5**, **9a**, **9b** and **10** [40,43,44]. The electronic effects of the addends are represented more exactly by comparing the [5,6]-carbosilylated adducts **9a**, **9b**, the [5,6]-pyrrolidino adduct **10** [44], and the [5,6]-tetracyanoethylene oxide (TCNEO) adduct **11** [45], which have the same addition patterns. As expected from the effects of the electron-donating silyl group and electron-withdrawing TCNEO moieties, the redox potentials of **9a**/**9b** and **11** shifted, respectively, to more negative and more positive potentials than those of reference compound **10**. Similar cathodic shifts of the redox potentials were observed for **6** and **7**, although the shift of $E^{ox}{}_1$ potential of **7** was somewhat smaller than expected for a disilirane adduct.

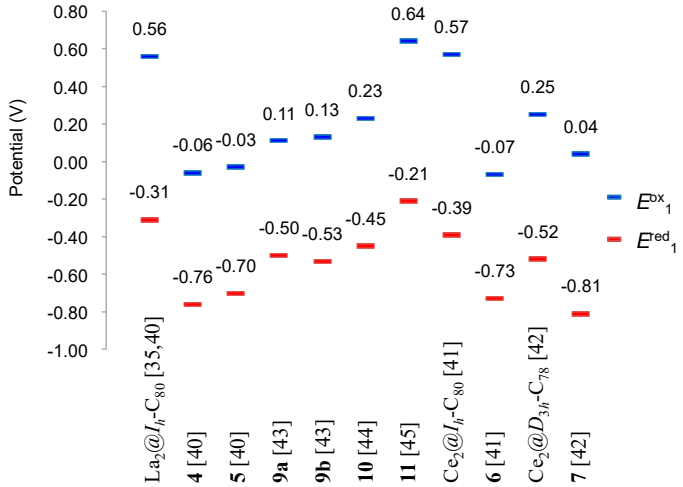


**Figure 3.** Redox potentials (in V vs. $Fc/Fc^+$) of pristine and derivatized dimetallofullerenes.

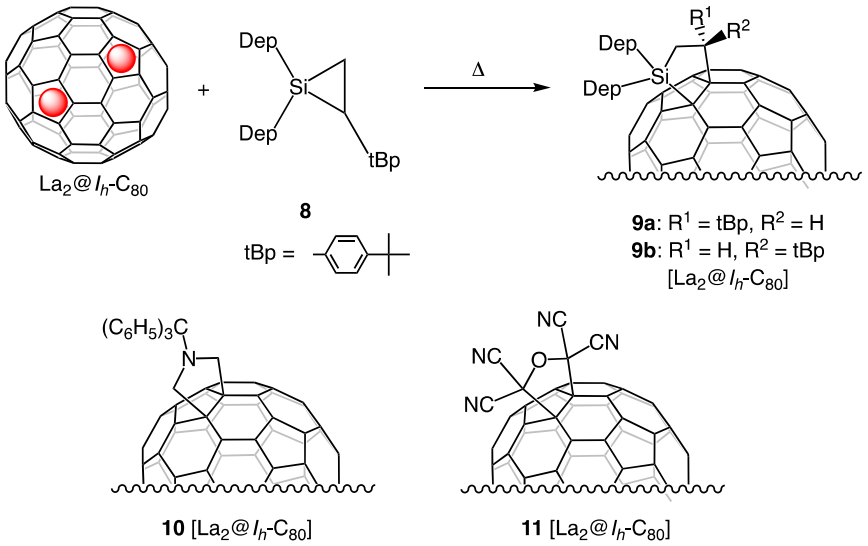


**Scheme 4.** Synthesis of silirane adducts of $La_2@I_h$-$C_{80}$. Partial structures are shown for **9a**, **9b**, **10** and **11**.

## 6. Reactions of $Sc_3N@I_h$-$C_{80}$ with Disilirane 1

Details of the structures and physical properties of silylated derivatives of $Sc_3N@I_h$-$C_{80}$, the most abundant trimetallic nitride template (TNT) fullerene, have been reported [37]. Irradiation of disilirane **1** and $Sc_3N@I_h$-$C_{80}$ in a mixed solvent of toluene/1,3,5-trichlorobenzene (3/1) produced the corresponding adducts, which were subsequently purified using HPLC to afford a mixture of two adducts **12a** and **12b** in a ratio of approximately 3:2 (Scheme 5). Although **12a** and **12b** could not be isolated, the NMR spectra of the mixture suggested that **12a** and **12b** consisted, respectively, of a 1,2-adduct at the [5,6]-junction, and a 1,4-adduct at the [5,6,6]-junctions on the $I_h$-$C_{80}$ cage. It is particularly interesting that when a mixture of **12a** and **12b** was heated in *o*-dichlorobenzene (ODCB) at 353 K, facile isomerization of **12a** to **12b** occurred, which suggests that **12b** is thermodynamically more stable than **12a**. The structure of **12b** was confirmed by X-ray crystallographic analysis to be the 1,4-adduct. Results also indicate the location of the encapsulated $Sc_3N$ cluster, which is oriented so that the Y-shaped $Sc_3N$ cluster straddles the addition site. Furthermore, theoretical calculations suggest that the free circular motion of the $Sc_3N$ cluster is restricted in **12b**. Similar addition patterns were reported for the 1,4-adducts, $Sc_3N@I_h$-$C_{80}(CF_3)_2$ [46] and $Sc_3N@I_h$-$C_{80}(CH_2C_6H_5)_2$ [47], which were synthesized, respectively, by radical addition reactions of $CF_3$ and $CH_2C_6H_5$ radicals.

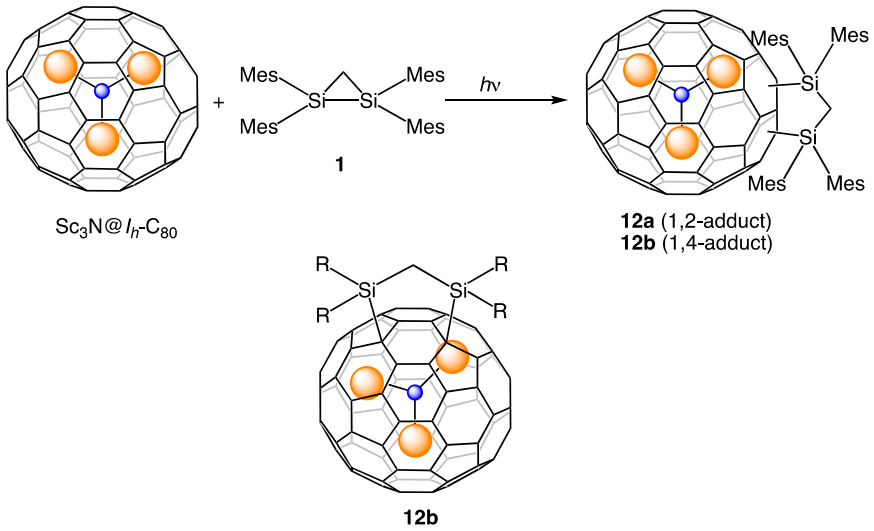


**Scheme 5.** Synthesis of disilirane adducts of $Sc_3N@I_h$-$C_{80}$.

The $E^{ox}{}_1$ and $E^{red}{}_1$ potentials of **12b** shifted remarkably to negative values by 540 and 230 mV, respectively, compared to those of pristine $Sc_3N@I_h$-$C_{80}$, reflecting the addition of two silyl groups (Figure 4). These shifts of the redox potentials correspond to changes in the lowest unoccupied molecular orbital (LUMO) and highest occupied molecular orbital (HOMO) levels according to theoretical calculations [37]. The HOMO and LUMO levels of **12b** are higher than those of pristine $Sc_3N@I_h$-$C_{80}$. In addition, the HOMO–LUMO energy gap of **12b** is smaller than that of $Sc_3N@I_h$-$C_{80}$. For comparison, the $E^{ox}{}_1$ and $E^{red}{}_1$ potentials of $Sc_3N@I_h$-$C_{80}(CF_3)_2$ were reported as +0.47 V and −1.16 V versus the ferrocene/ferrocenium couple ($Fc/Fc^+$), respectively, in agreement with the electron-withdrawing effects of the $CF_3$ groups [46].

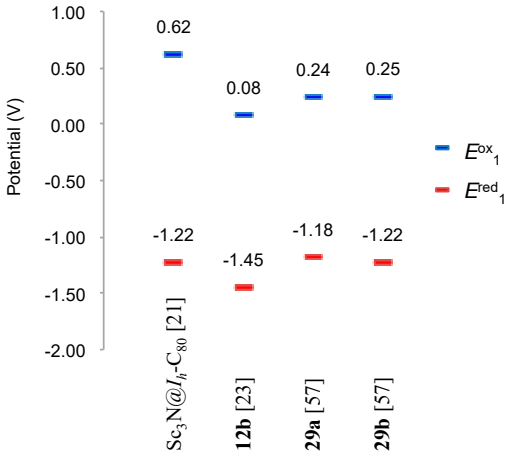


**Figure 4.** Redox potentials (in V vs. $Fc/Fc^+$) of pristine and derivatized $Sc_3N@I_h$-$C_{80}$.

## 7. Reactions of $Lu_3N@I_h$-$C_{80}$ with Silylene

In recent years, among the TNT EMFs, $Lu_3N@I_h$-$C_{80}$ has emerged as a suitable acceptor for organic solar cells because the LUMO level of $Lu_3N@I_h$-$C_{80}$ is higher than that of $C_{60}$ and other TNT EMFs, $M_3N@I_h$-$C_{80}$ (M = Sc, Y, etc.) [48,49]. Indeed, methano-bridged derivatives of $Lu_3N@I_h$-$C_{80}$ have been synthesized for application in organic photovoltaic (OPV) devices, which show increases in open circuit voltage and higher efficiencies. For the application of EMFs to OPV devices, the silylation

reaction is attractive to adjust the LUMO levels of the EMFs. These results prompted us to investigate the synthesis and properties of organosilicon derivatives of $Lu_3N@I_h$-$C_{80}$.

Previously, the addition of silylene to $C_{60}$ was achieved by photochemical reactions using trisilane compounds **13** [50] as precursors of silylenes (Scheme 6). However, this reaction requires short-wavelength ultraviolet irradiation using low-pressure mercury lamps. When a solution of $Lu_3N@I_h$-$C_{80}$ and **13** was photolyzed via ultraviolet irradiation, no silylene adduct was obtained, whereas $Lu_3N@I_h$-$C_{80}$ was consumed. This result indicates that ultraviolet irradiation is unsuitable for silylene addition reactions of EMFs. Therefore, we synthesized bicyclic silirane **14** as an alternative silylene precursor, which extrudes **15** under thermal reaction conditions [51]. An ODCB solution of **14** and $Lu_3N@I_h$-$C_{80}$ was heated in the dark to afford two silylene mono-adducts **16a** and **16b** (Scheme 6). Based on NMR analysis, the structures of **16a** and **16b** were determined respectively to be [5,6]- and [6,6]-adducts. Furthermore, the fulleroid structure of **16a** was established via X-ray crystallographic analysis. Adducts **16a** and **16b** were sensitive to ambient light. They decomposed gradually to afford pristine $Lu_3N@I_h$-$C_{80}$. In addition, the isomerization of **16b** to **16a** was also observed upon exposure to ambient light. In contrast, in the addition of silylene to $Sc_3N@I_h$-$C_{80}$ using **14** under the same conditions, the reaction was not efficient. It afforded a poor product yield, preventing further structural elucidation. Based on the electrophilic character of silylenes, the HOMOs of $M_3N@I_h$-$C_{80}$ (M = Sc and Lu) might play an important role in their different reactivities toward **15**.

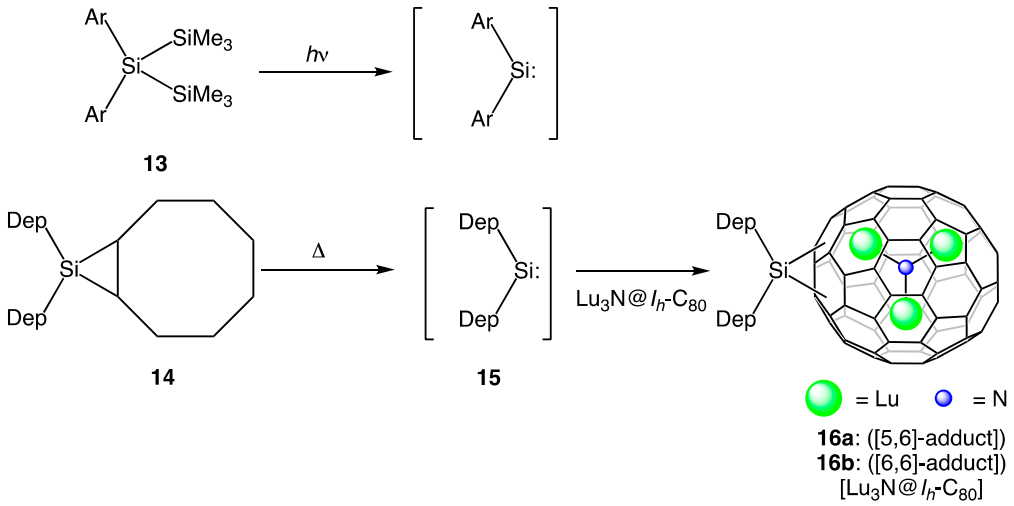


**Scheme 6.** Synthesis of silylene adducts of $Lu_3N@I_h$-$C_{80}$.

Electrochemical measurements yielded the voltammograms of **16a** and **16b**, which showed irreversible oxidation and reduction processes. The formation of pristine $Lu_3N@I_h$-$C_{80}$ was observed from electrochemical measurements [51]. The $E^{ox}{}_1$ potentials of **16a** and **16b** shifted toward more negative values by 340 and 180 mV, respectively, compared with those of $Lu_3N@I_h$-$C_{80}$ (Figure 5). However, the cathodic shifts of the $E^{red}{}_1$ potentials of **16a** and **16b** were observed to be 40 and 130 mV, respectively, relative to that of $Lu_3N@I_h$-$C_{80}$. As observed for **16a** and **16b**, the redox behaviors of derivatized EMFs depend on the addition pattern on the carbon cages. The redox potentials of **16a** and **16b** were also compared with those of the [6,6]-Bingel–Hirsch derivatives **17** [52], **18** [52], **19** [53], the [6,6]-carbene adduct **20** [54], and the [5,6]-carbene adduct **21** [54] (Figure 6). The $E^{ox}{}_1$ values of the **17**–**21** were shifted less cathodically than those of **16a** and **16b**, indicating that the addition of silylenes raises the HOMO levels of the products. In addition, the cathodic shifts of the $E^{red}{}_1$ values of the [6,6]-adduct **16b** and the [5,6]-adduct **16a** are 130 and 40 mV, respectively, compared to that of $Lu_3N@I_h$-$C_{80}$. It is noteworthy that those shifts of **17**–**19** ([6,6]-adducts) are 30–160 mV, while that of **21** ([5,6]-adduct) is 70 mV [52–54].

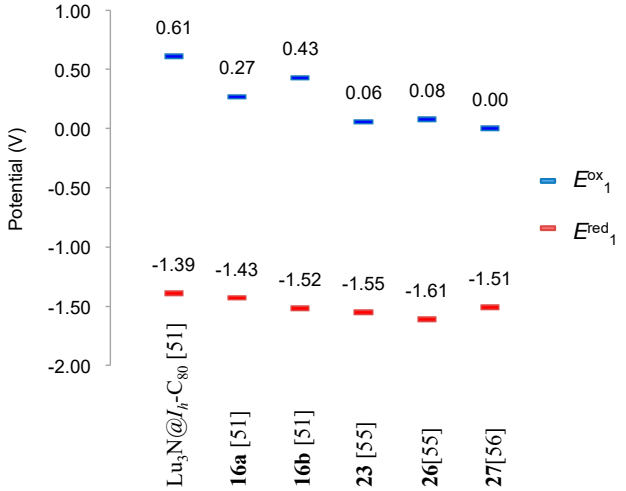


**Figure 5.** Redox potentials (in V vs. $Fc/Fc^+$) of pristine and derivatized $Lu_3N@I_h$-$C_{80}$.

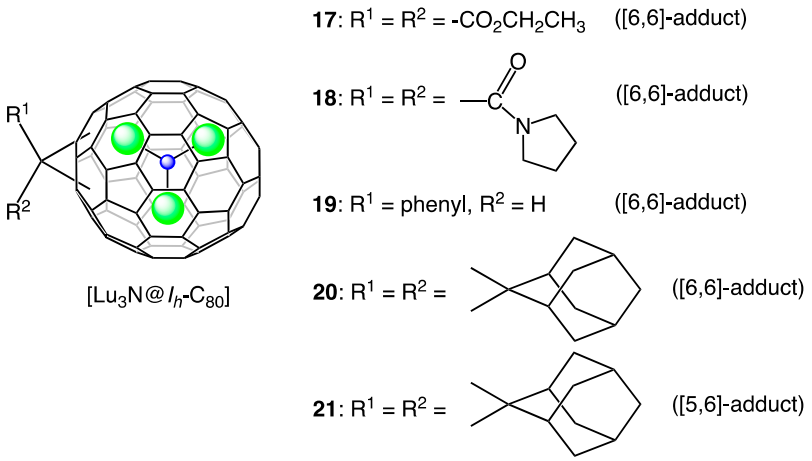


**Figure 6.** Structures of **17**–**21**.

## 8. Reactions of $Lu_3N@I_h$-$C_{80}$ with Disilirane and Digermirane

The electronic effects of silylene on the redox properties of EMFs were found to be moderate, as observed for **16a** and **16b**. Therefore, the reactions between $Lu_3N@I_h$-$C_{80}$ and disiliranes **1** and **2** were investigated to evaluate the electronic effects of bis-silylation on pristine $Lu_3N@I_h$-$C_{80}$ [55]. Photoreaction of $Lu_3N@I_h$-$C_{80}$ and disilirane **1** (or **2**) was conducted in a mixed solvent of ODCB/toluene using halogen–tungsten lamps. As shown in Scheme 7, the reaction of **1** afforded **22** and **23**, whereas that of **2** afforded **24**, **25**, and **26**, respectively, as 1:1 adducts of $Lu_3N@I_h$-$C_{80}$ and disiliranes. In addition, **22**, **24**, and **25** were found to be unstable; **22** readily isomerized to **23**, whereas **24** and **25** isomerized to **26**. Therefore, elucidation of the structures and physical properties of **22**, **24**, and **25** has been hitherto unsuccessful. The stable adducts **23** and **26** were determined to be the 1,4-adducts on the [5,6,6]-junctions of the $I_h$-$C_{80}$ cage via single X-ray crystallographic analysis [56].

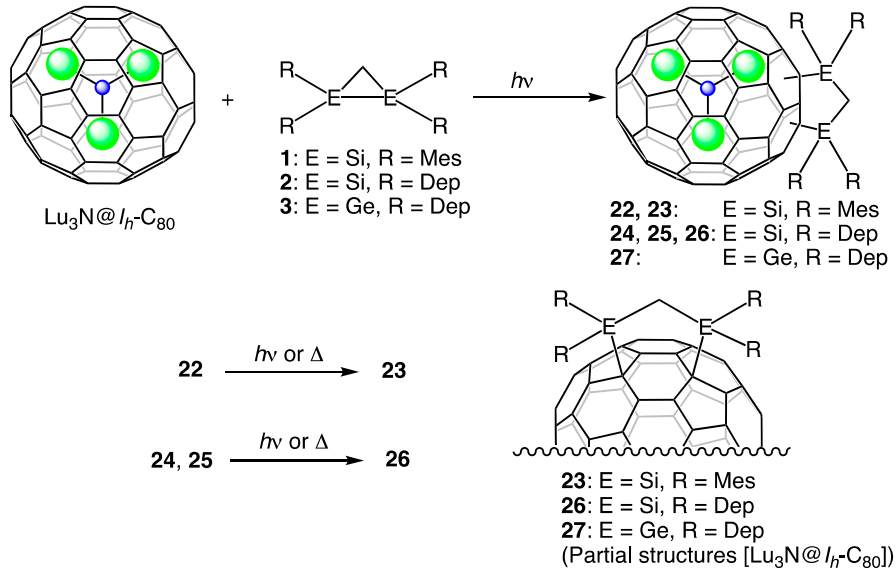


**Scheme 7.** Synthesis of disilirane and digermirane adducts of $Lu_3N@I_h$-$C_{80}$, and isomerization reactions of **22**, **24** and **25**.

Furthermore, the photoreaction of $Lu_3N@I_h$-$C_{80}$ with digermirane **3** was investigated to compare the electronic properties of the germylated and silylated derivatives [56]. Due to the higher orbital energy levels of C–Ge bonds compared to those of C–Si bonds, it is expected that germylation will perturb the electronic properties of fullerenes effectively. It is particularly interesting that the photoreaction of $Lu_3N@I_h$-$C_{80}$ with **3** proceeded faster than with **2** to afford the corresponding 1,4-adduct **27** under the same reaction conditions (Scheme 7). The structure of **27** was also confirmed using X-ray crystallographic analysis. Results of our earlier study demonstrate that $C_{60}$ functions as an electron acceptor in the photoreactions with **1** [25]. Therefore, a similar electron donor–acceptor interaction is presumed to occur in the case of $Lu_3N@I_h$-$C_{80}$. In fact, the high electron donating property of **3** is explained respectively based on the oxidation peak potentials of **2** (+0.54 V) and **3** (+0.45 V) relative to the $Fc/Fc^+$ couple. This result was also supported by comparison of the HOMO levels of **2** and **3** obtained using theoretical calculations. Furthermore, the calculated structures of **2** and **3** indicate that the Ge–Ge and Ge–C bonds of **3** are slightly longer, respectively, than the Si–Si and Si–C bonds of **2**. As expected, the high reactivity of **3** can be attributed to its good electron donor properties and its low steric hindrance around the Ge–Ge bond [56].

From electrochemical measurements of **23**, **26** and **27**, both oxidation and reduction processes were found to be irreversible. Figure 5 shows that the $E^{ox}{}_1$ values of **23**, **26**, and **27** shifted to more negative potentials by 530 to 610 mV, compared with that of pristine $Lu_3N@I_h$-$C_{80}$. Cathodic shifts of $E^{red}{}_1$ values were also observed for **23**, **26**, and **27** within the range of 120 to 220 mV. The $E^{ox}{}_1$ and $E^{red}{}_1$ values of **27** showed slight cathodic and anodic shifts, respectively, compared to the corresponding redox potentials of **23** and **26**. As a result, **27** was found to be oxidized and reduced more readily than **23** or **26**. These cathodic shifts of $E^{ox}{}_1$ values of **23**, **26** and **27** were confirmed to be remarkably larger than those of **16a** and **16b**, as expected from the number of silicon and germanium atoms introduced into the fullerene cages.

## 9. Reactions of $Sc_3N@I_h$-$C_{80}$ with Silirane 28

As described above, the addition reaction between $Sc_3N@I_h$-$C_{80}$ and silylene produced the corresponding adduct in poor yield. This result prompted us to develop an alternative silylation reaction of $Sc_3N@I_h$-$C_{80}$ using silirane **28** [57]. Photoirradiation of a toluene solution of $Sc_3N@I_h$-$C_{80}$ and **28** afforded three compounds **29a**, **29b**, and **29c** (Scheme 8). Results of MALDI-TOF mass spectrometry, VIS-NIR and NMR spectroscopy suggest that **29a** and **29b** are a pair of diastereomers

of [5,6]-adducts, whereas **29c** might be a [6,6]-adduct. However, further characterization of **29c** has not yet been achieved because of its low yield. It is noteworthy that the carbosilylation of $La_2@I_h$-$C_{80}$ using **8** was conducted under thermal conditions. However, the reaction of $La_2@I_h$-$C_{80}$ using **8** did not proceed efficiently under photolytic conditions [43].

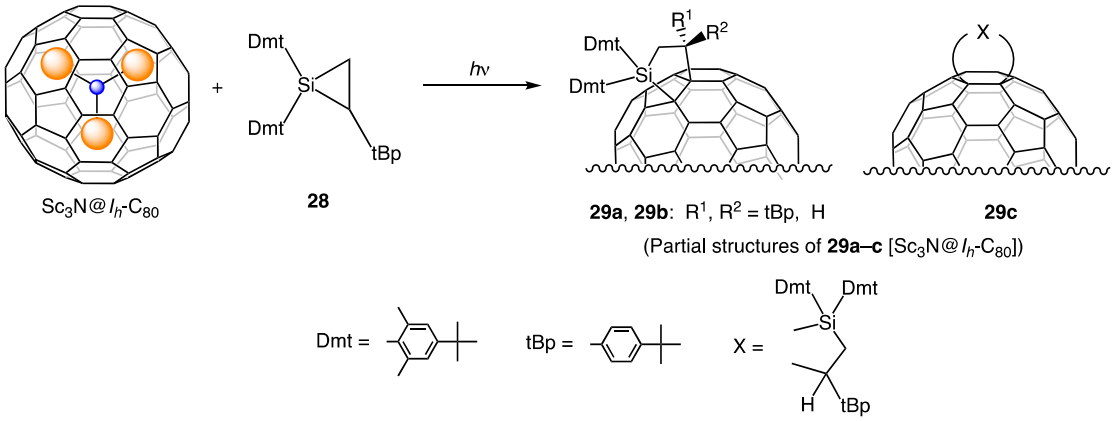


**Scheme 8.** Synthesis of silirane adducts of $Sc_3N@I_h$-$C_{80}$.

The $E^{ox}{}_1$ values of **29a** and **29b** shifted toward more negative potentials by 380 and 370 mV, respectively, relative to that of $Sc_3N@I_h$-$C_{80}$ (Figure 4). However, the $E^{red}{}_1$ values of **29a** and **29b** were nearly equal to that of $Sc_3N@I_h$-$C_{80}$. These properties were verified based on the HOMO and LUMO energies of **29a** and **29b** obtained using theoretical calculations. To confirm the electronic effects of carbosilylation, these values were evaluated by comparing with those of the [5,6]-pyrrolidino adducts **30a** [58], **30b** [58], and **31** [59,60], and the [5,6]-benzyne adduct **32** [61] (Figure 7). Results show that both the $E^{ox}{}_1$ and $E^{red}{}_1$ potentials of **29a** and **29b** were shifted slightly toward more negative values than those of **30a**, **30b**, **31** and **32**. By coupling the redox properties of **9a** and **9b**, it appears that carbosilylation of EMFs produces slight cathodic shifts of the redox potentials compared to those produced by derivatization with carbon-based addends.

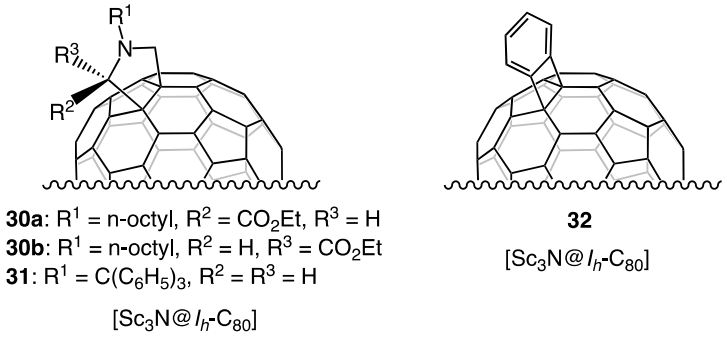


**Figure 7.** Partial structures of **30a**, **30b**, **31** and **32**.

## 10. Dynamic Behaviors of the Encapsulated Atoms

The behavior of encapsulated metal atoms is an interesting issue affecting chemical and physical properties of EMFs. The movements of encapsulated metal atoms are affected by both the electrostatic metal–cage and the metal–metal interactions. In the case of monometallic EMF, metal atoms tend not to move around inside the cages. In dimetallofullerenes with highly-symmetric carbon cages, such as $M_2@I_h$-$C_{80}$, two atoms can rotate in every direction along the endohedral surface [62–65]. However, the positions and behaviors of metal atoms, as well as their electronic properties, were found to be altered by exohedral derivatization. For example, the encapsulated Ce atoms in **6** were

observed to be fixed at two positions close to the six-membered ring on the equator of the $I_h$-$C_{80}$ cage via X-ray crystallographic and paramagnetic $^{13}$C-NMR spectral analysis [41]. In addition, variable temperature (VT) $^{139}$La NMR and X-ray crystallographic analysis of **5** revealed that the La atoms circulate two-dimensionally along the equator of the $C_{80}$ cage [40]. These results were consistent with earlier reported results of theoretical calculations [66].

The dynamic behaviors of the encapsulated metal atoms in **9a** and **9b** were also studied using VT $^{139}$La NMR spectroscopy and theoretical calculations [43]. The results showed that the line width of the $^{139}$La signal is broadened at temperatures higher than 280 K, suggesting that the two La atoms move dynamically inside the carbon cage of **9a** and **9b**. Coupling of these results with the X-ray crystallographic analysis of **9a** suggests that the La atoms are moving inside an annular belt formed from the six-membered rings [43].

## 11. Potential Applications

As shown in this review, various EMFs and empty fullerenes showed high reactivities toward disiliranes, which have activated Si–Si bonds. Moreover, polysilanes, i.e., polymers comprising of catenated Si–Si bonds as polymer backbones, have attracted considerable interest as novel functional materials because of their unique chemical and physical properties [67,68]. Based on the delocalization of σ–electrons along the backbones of polysilanes, they have been studied as future functional materials, such as conductive polymers [69–78], photoresists [79], and organic light emitting diodes (LEDs) [80]. Polysilanes are well-known for their high hole mobility, however, their photoinduced charge carrier generation is not efficient. Doping $C_{60}$ as an acceptor into polysilanes resulted in photoinduced electron transfer between them, which dramatically improved the charge carrier generation efficiency [70,71]. The electron transfer processes between photoexcited $C_{60}$ and polysilanes [81,82] or polygermanes [83] were confirmed by laser flash photolysis experiments.

Due to their photoconductive properties, polysilanes may be applied to novel organic semiconductor devices. Some researchers investigated the photovoltaic properties of bulk heterojunction solar cells using $C_{60}$ and [6,6]-phenyl $C_{61}$-butyric acid methyl ester (PCBM) as electron acceptors and polysilanes as electron donors [84–87]. Furthermore, composite materials composed of polysilanes and EMFs may exhibit improved electronic properties as compared with those of empty fullerene-based materials. The organic solar cells using $Lu_3N@I_h$-$C_{80}$ as an acceptor material showed higher open circuit voltages and higher photovoltaic efficiencies than those of $C_{60}$ because of the higher LUMO level of $Lu_3N@I_h$-$C_{80}$ [48,49].

The MO levels of the silylated and germylated EMFs were remarkably altered by the electron donating silyl and germyl groups as compared with those of pristine EMFs. Therefore, silylation and germylation would be useful for adjusting the electronic properties of EMF derivatives in electronic devices. In addition, covalent bonding between fullerenes and polysilanes can be used to construct donor–acceptor conjugate structures. The first prototype polysilane that incorporated $C_{60}$ into the polymer backbone was synthesized by the photoreaction of a polysilane with $C_{60}$ [88–91]. Development of silylation and germylation reactions of fullerenes will provide useful methods for affording fullerene-polysilane/polygermane conjugates.

## 12. Summary

This review provided an overview of our studies of the synthesis and characterization of silylated and germylated derivatives of EMFs using active silicon compounds and germanium compounds. Among these, disilirane **1** has been used as a versatile substrate that is both photochemically and thermally reactive. A comparison of the redox potentials of EMFs revealed that the reactivities of EMFs toward **1** depend on the electron-accepting abilities of the EMFs. Moreover, NMR and X-ray crystallographic examinations revealed that silylation affects the dynamic behavior of the encapsulated metal atoms and clusters in the EMFs. For example, results show that the movement of the La atoms in $La_2@I_h$-$C_{80}$ was restricted to two-dimensional rotation near the equatorial plane of the carbon

cage upon addition of **1**. The electronic effects of silylation and germylation on EMFs were clarified by electrochemical examinations and theoretical calculations. In general, the redox potentials of silylated and germylated derivatives shifted to more negative values relative to those of pristine EMFs. In particular, the cathodic shifts of the oxidation potentials were found to be remarkably large, reflecting the electron-donating effects of the silyl and germyl groups. These results demonstrate that EMFs with novel physical properties and functionalities are obtainable through chemical modification by exploiting the properties of various heteroatom-based functional groups.

**Acknowledgments:** This work was supported by a Grant-in-Aid for Scientific Research on Innovative Areas (No. 20108001, "pi-Space"), a Grant-in-Aid for Scientific Research (A) (No. 202455006), (B) (No. 24350019), and (C) (No. 17K05797), and Specially Promoted Research (No. 22000009) from the Ministry of Education, Culture, Sports, Science, and Technology of Japan.

**Conflicts of Interest:** The authors declare no conflict of interest.

## References

1. *Endofullerenes: A New Family of Carbon Clusters*; Akasaka, T., Nagase, S., Eds.; Kluwer: Dordrecht, The Netherlands, 2002.
2. Dunsch, L.; Yang, S. Metal nitride cluster fullerenes: Their current state and future prospects endohedral fullerenes. *Small* **2007**, *8*, 1298–1320. [CrossRef] [PubMed]
3. Chaur, M.N.; Melin, F.; Ortiz, A.L.; Echegoyen, L. Chemical, electrochemical, and structural properties of endohedral metallofullerenes. *Angew. Chem. Int. Ed.* **2009**, *48*, 7514–7538. [CrossRef] [PubMed]
4. Yamada, M.; Akasaka, T.; Nagase, S. Endohedral metal atoms in pristine and functionalized fullerene cages. *Acc. Chem. Res.* **2010**, *43*, 92–102. [CrossRef] [PubMed]
5. *Chemistry of Nanocarbons*; Akasaka, T., Wudl, F., Nagase, S., Eds.; Wiley: Chichester, UK, 2010.
6. Maeda, Y.; Tsuchiya, T.; Lu, X.; Takano, Y.; Akasaka, T.; Nagase, S. Current progress on the chemical functionalization and supramolecular chemistry of M@$C_{82}$. *Nanoscale* **2011**, *3*, 2421–2429. [CrossRef] [PubMed]
7. Lu, X.; Akasaka, T.; Nagase, S. Chemistry of endohedral metallofullerenes: The role of metals. *Chem. Commun.* **2011**, *47*, 5942–5957. [CrossRef] [PubMed]
8. Lu, X.; Feng, L.; Akasaka, T.; Nagase, S. Current status and future developments of endohedral metallofullerenes. *Chem. Soc. Rev.* **2012**, *41*, 7723–7760. [CrossRef] [PubMed]
9. Zhang, J.; Stevenson, S.; Dorn, H.C. Trimetallic nitride template endohedral metallofullerenes: Discovery, structural characterization, reactivity, and applications. *Acc. Chem. Res.* **2013**, *46*, 1458–1557. [CrossRef] [PubMed]
10. Rivera-Nazario, D.M.; Pinzón, J.R.; Stevenson, S.; Echegoyen, L.A. Buckyball maracas: Exploring the inside and outside properties of endohedral fullerenes. *J. Phys. Org. Chem.* **2013**, *26*, 194–205. [CrossRef]
11. Yamada, M.; Akasaka, T.; Nagase, S. Carbene additions to fullerenes. *Chem. Rev.* **2013**, *113*, 7209–7264. [CrossRef] [PubMed]
12. Lu, X.; Akasaka, T.; Nagase, S. Carbide cluster metallofullerenes: Structure, properties, and possible origin. *Acc. Chem. Res.* **2013**, *46*, 1627–1635. [CrossRef] [PubMed]
13. Popov, A.A.; Yang, S.; Dunsch, L. Endohedral fullerenes. *Chem. Rev.* **2013**, *113*, 5989–6113. [CrossRef] [PubMed]
14. Nagase, S. Theory and calculations of molecules containing heavier main group elements and fullerenes encaging transition metals: Interplay with experiment. *Bull. Chem. Soc. Jpn.* **2014**, *87*, 167–195. [CrossRef]
15. Yamada, M.; Akasaka, T. Emergence of highly elaborated $\pi$-space and extending its functionality based on nanocarbons: New vistas in the fullerene world. *Bull. Chem. Soc. Jpn.* **2014**, *87*, 1289–1314. [CrossRef]
16. Bock, H.; Solouki, B. Photoelectron spectra of silicon compounds. In *The Chemistry of Organosilicon Compounds*; Patai, S., Rappoport, Z., Eds.; Wiley: Chichester, UK, 1989; Part 1, Chapter 9, pp. 555–653.
17. Traylor, T.G.; Hanstein, W.; Berwin, H.J.; Clinton, N.A.; Brown, R.S. Vertical stabilization of cations by neighboring $\sigma$ bonds. General considerations. *J. Am. Chem. Soc.* **1971**, *93*, 5715–5725. [CrossRef]
18. Hosomi, A. Characteristics in the reactions of allylsilanes and their applications to versatile synthetic equivalents. *Acc. Chem. Res.* **1988**, *21*, 200–206. [CrossRef]

19. Fleming, I.; Barbero, A.; Walter, D. Stereochemical control in organic synthesis using silicon-containing compounds. *Chem. Rev.* **1997**, *97*, 2063–2192. [CrossRef] [PubMed]
20. Akasaka, T.; Ando, W.; Kobayashi, K.; Nagase, S. Reaction of $C_{60}$ with silylene, the first fullerene silirane derivative. *J. Am. Chem. Soc.* **1993**, *115*, 1605–1606. [CrossRef]
21. Akasaka, T.; Ando, W.; Kobayashi, K.; Nagase, S. Photochemical [2 + 3] cycloaddition of $C_{60}$ with disilirane. *J. Am. Chem. Soc.* **1993**, *115*, 10366–10367. [CrossRef]
22. Suzuki, T.; Maruyama, Y.; Akasaka, T.; Ando, W.; Kobayashi, K.; Nagase, S. Redox properties of organofullerenes. *J. Am. Chem. Soc.* **1994**, *116*, 1359–1363. [CrossRef]
23. Akasaka, T.; Mitsuhida, E.; Ando, W.; Kobayashi, K.; Nagase, S. Adduct of $C_{70}$ at the equatorial belt: Photochemical cycloaddition with disilirane. *J. Am. Chem. Soc.* **1994**, *116*, 2627–2628. [CrossRef]
24. Akasaka, T.; Mitsuhida, E.; Ando, W.; Kobayashi, K.; Nagase, S. Regioselective addition of silylene onto [70] fullerene. *J. Chem. Soc. Chem. Commun.* **1995**, 1529–1530. [CrossRef]
25. Akasaka, T.; Maeda, Y.; Wakahara, T.; Okamura, M.; Fujitsuka, M.; Ito, O.; Kobayashi, K.; Nagase, S.; Kako, M.; Nakadaira, Y.; et al. Novel Metal-free bis-silylation: $C_{60}$-sensitized reaction of disilirane with benzonitrile. *Org. Lett.* **1999**, *1*, 1509–1512. [CrossRef]
26. Akasaka, T.; Suzuki, T.; Maeda, Y.; Ara, M.; Wakahara, T.; Kobayashi, K.; Nagase, S.; Kako, M.; Nakadaira, Y.; Fujitsuka, M.; et al. Photochemical bissilylation of $C_{60}$ with disilane. *J. Org. Chem.* **1999**, *64*, 566–569. [CrossRef]
27. Han, A.; Wakahara, T.; Maeda, Y.; Niino, Y.; Akasaka, T.; Yamamoto, K.; Kako, M.; Nakadaira, Y.; Kobayashi, K.; Nagase, S. Photochemical cycloaddition of $C_{78}$ with disilirane. *Chem. Lett.* **2001**, 974–975. [CrossRef]
28. Wakahara, T.; Han, A.; Niino, Y.; Maeda, Y.; Akasaka, T.; Suzuki, T.; Yamamoto, K.; Kako, M.; Nakadaira, Y.; Kobayashi, K.; et al. Silylation of higher fullerenes. *J. Mater. Chem.* **2002**, *12*, 2061–2064. [CrossRef]
29. Maeda, Y.; Rahman, G.M.A.; Wakahara, T.; Kako, M.; Okamura, M.; Sato, S.; Akasaka, T.; Kobayashi, K.; Nagase, S. Synthesis and characterization of tetrakis-silylated $C_{60}$ isomers. *J. Org. Chem.* **2003**, *68*, 6791–6794. [CrossRef] [PubMed]
30. Han, A.H.; Wakahara, T.; Maeda, Y.; Akasaka, T.; Fujitsuka, M.; Ito, O.; Yamamoto, K.; Kako, M.; Kobayashi, K.; Nagase, S. A new method for separating the $D_3$ and $C_{2v}$ isomers of $C_{78}$. *New J. Chem.* **2009**, *33*, 497–500. [CrossRef]
31. Wakahara, T.; Kako, M.; Maeda, Y.; Akasaka, T.; Kobayashi, K.; Nagase, S. Synthesis and characterization of cyclic silicon compounds of fullerenes. *Curr. Org. Chem.* **2003**, *7*, 927–943. [CrossRef]
32. Nagatsuka, J.; Sugitani, S.; Kako, M.; Nakahodo, T.; Mizorogi, N.; Ishitsuka, M.O.; Maeda, Y.; Tsuchiya, T.; Akasaka, T.; Gao, X.; et al. Photochemical addition of $C_{60}$ with siliranes: Synthesis and characterization of carbosilylated and hydrosilylated $C_{60}$ derivatives. *J. Am. Chem. Soc.* **2010**, *132*, 12106–12120. [CrossRef] [PubMed]
33. Akasaka, T.; Kato, T.; Kobayashi, K.; Nagase, S.; Yamamoto, K.; Funasaka, H.; Takahashi, T. Exohedral adducts of La@$C_{82}$. *Nature* **1995**, *374*, 600–601. [CrossRef]
34. Akasaka, T.; Kato, T.; Nagase, S.; Kobayashi, K.; Yamamoto, K.; Funasaka, H.; Takahashi, T. Chemical derivatization of endohedral metallofullerene La@$C_{82}$ with digermirane. *Tetrahedron* **1996**, *52*, 5015–5020. [CrossRef]
35. Akasaka, T.; Nagase, S.; Kobayashi, K.; Suzuki, T.; Kato, T.; Kikuchi, K.; Achiba, Y.; Yamamoto, K.; Funasaka, H.; Takahashi, T. Synthesis of the first adducts of the dimetallofullerenes $La_2$@$C_{80}$ and $Sc_2$@$C_{84}$ by addition of a disilirane. *Angew. Chem. Int. Ed.* **1995**, *34*, 2139–2141. [CrossRef]
36. Iiduka, Y.; Ikenaga, O.; Sakuraba, A.; Wakahara, T.; Tsuchiya, T.; Maeda, Y.; Nakahodo, T.; Akasaka, T.; Kako, M.; Mizorogi, N.; et al. Chemical reactivity of $Sc_3N$@$C_{80}$ and $La_2$@$C_{80}$. *J. Am. Chem. Soc.* **2005**, *127*, 9956–9957. [CrossRef] [PubMed]
37. Wakahara, T.; Iiduka, Y.; Ikenaga, O.; Nakahodo, T.; Sakuraba, A.; Tsuchiya, T.; Maeda, Y.; Kako, M.; Akasaka, T.; Yoza, K.; et al. Characterization of the bis-silylated endofullerene $Sc_3N$@$C_{80}$. *J. Am. Chem. Soc.* **2006**, *128*, 9919–9925. [CrossRef] [PubMed]
38. Maeda, Y.; Miyashita, J.; Hasegawa, T.; Wakahara, T.; Tsuchiya, T.; Feng, L.; Lian, Y.; Akasaka, T.; Kobayashi, K.; Nagase, S.; et al. Chemical reactivities of the cation and anion of M@$C_{82}$ (M = Y, La, and Ce). *J. Am. Chem. Soc.* **2005**, *127*, 2143–2146. [CrossRef] [PubMed]

39. Yamada, M.; Feng, L.; Wakahara, T.; Tsuchiya, T.; Maeda, Y.; Lian, Y.; Kako, M.; Akasaka, T.; Kato, T.; Kobayashi, K.; et al. Synthesis and characterization of exohedrally silylated M@$C_{82}$ (M = Y and La). *J. Phys. Chem. B* **2005**, *109*, 6049–6051. [CrossRef] [PubMed]
40. Wakahara, T.; Yamada, M.; Takahashi, S.; Nakahodo, T.; Tsuchiya, T.; Maeda, Y.; Akasaka, T.; Kako, M.; Yoza, K.; Horn, E.; et al. Two-dimensional hopping motion of encapsulated La atoms in silylated $La_2$@$C_{80}$. *Chem. Commun.* **2007**, 2680–2682. [CrossRef] [PubMed]
41. Yamada, M.; Wakahara, T.; Tsuchiya, T.; Maeda, Y.; Akasaka, T.; Kako, M.; Yoza, K.; Horn, E.; Mizorogi, N.; Kobayashi, K.; et al. Positional control of encapsulated atoms inside a fullerene cage by exohedral addition. *J. Am. Chem. Soc.* **2005**, *127*, 14570–14571. [CrossRef] [PubMed]
42. Yamada, M.; Wakahara, T.; Tsuchiya, T.; Maeda, Y.; Kako, M.; Akasaka, T.; Yoza, K.; Horn, E.; Mizorogi, N.; Nagase, S. Location of the metal atoms in $Ce_2$@$C_{78}$ and its bis-silylated derivative. *Chem. Commun.* **2008**, 558–560. [CrossRef] [PubMed]
43. Yamada, M.; Minowa, M.; Sato, S.; Kako, M.; Slanina, Z.; Mizorogi, N.; Tsuchiya, T.; Maeda, Y.; Nagase, S.; Akasaka, T. Thermal carbosilylation of endohedral dimetallofullerene $La_2$@$I_h$-$C_{80}$ with silirane. *J. Am. Chem. Soc.* **2010**, *132*, 17953–17960. [CrossRef] [PubMed]
44. Yamada, M.; Wakahara, T.; Nakahodo, T.; Tsuchiya, T.; Maeda, Y.; Akasaka, T.; Yoza, K.; Horn, E.; Mizorogi, N.; Nagase, S. Synthesis and structural characterization of endohedral pyrrolidinodimetallofullerene: $La_2$@$C_{80}$ $(CH_2)_2$*N*Trt. *J. Am. Chem. Soc.* **2006**, *128*, 1402–1403. [CrossRef] [PubMed]
45. Yamada, M.; Minowa, M.; Sato, S.; Slanina, Z.; Tsuchiya, T.; Maeda, Y.; Nagase, S.; Akasaka, T. Regioselective cycloaddition of $La_2$@$I_h$-$C_{80}$ with tetracyanoethylene oxide: Formation of an endohedral dimetallofullerene adduct featuring enhanced electron-accepting character. *J. Am. Chem. Soc.* **2011**, *133*, 3796–3799. [CrossRef] [PubMed]
46. Shustova, N.B.; Popov, A.A.; Mackey, M.A.; Coumbe, C.E.; Phillips, J.P.; Stevenson, S.; Strauss, S.H.; Boltalina, O.V. Radical trifluoromethylation of $Sc_3N$@$C_{80}$. *J. Am. Chem. Soc.* **2007**, *129*, 11676–11677. [CrossRef] [PubMed]
47. Shu, C.Y.; Slebodnick, C.; Xu, L.S.; Champion, H.; Fuhrer, T.; Cai, T.; Reid, J.E.; Fu, W.; Harich, K.; Dorn, H.C.; et al. Highly Regioselective derivatization of trimetallic nitride templated endohedral metallofullerenes via a facile photochemical reaction. *J. Am. Chem. Soc.* **2008**, *130*, 17755–17760. [CrossRef] [PubMed]
48. Ross, R.B.; Cardona, C.M.; Guldi, D.M.; Sankaranarayanan, S.G.; Reese, M.O.; Kopidakis, N.; Peet, J.; Walker, B.; Bazan, G.C.; Van Keuren, E.; et al. Endohedral fullerenes for organic photovoltaic devices. *Nat. Mater.* **2009**, *8*, 208–212. [CrossRef] [PubMed]
49. Ross, R.B.; Cardona, C.M.; Swain, F.B.; Guldi, D.M.; Sankaranarayanan, S.G.; Van Keuren, E.; Holloway, B.C.; Drees, M. Tuning conversion efficiency in metallo endohedral fullerene-based organic photovoltaic devices. *Adv. Funct. Mater.* **2009**, *19*, 2332–2337. [CrossRef]
50. Gaspar, P.P.; West, R. Silylenes. In *The Chemistry of Organosilicon Compounds*; Rappoport, Z., Apeloig, Y., Eds.; Wiley: Chichester, UK, 1998; Volume 2, Part 3, Chapter 43, pp. 2463–2568.
51. Sato, K.; Kako, M.; Suzuki, M.; Mizorogi, N.; Tsuchiya, T.; Olmstead, M.M.; Balch, A.L.; Akasaka, T.; Nagase, S. Synthesis of silylene-bridged endohedral metallofullerene $Lu_3N$@$I_h$-$C_{80}$. *J. Am. Chem. Soc.* **2012**, *134*, 16033–16039. [CrossRef] [PubMed]
52. Pinzón, J.R.; Zuo, T.; Echegoyen, L. Synthesis and electrochemical studies of Bingel–Hirsch derivatives of $M_3N$@$I_h$-$C_{80}$ (M = Sc, Lu). *Chem. Eur. J.* **2010**, *16*, 4864–4869. [CrossRef] [PubMed]
53. Li, F.F.; Rodríguez-Fortea, A.; Poblet, J.M.; Echegoyen, L. Reactivity of metallic nitride endohedral metallofullerene anions: Electrochemical synthesis of a $Lu_3N$@$I_h$-$C_{80}$ derivative. *J. Am. Chem. Soc.* **2011**, *133*, 2760–2765. [CrossRef] [PubMed]
54. Yamada, M.; Abe, T.; Saito, C.; Yamazaki, T.; Sato, S.; Mizorogi, N.; Slanina, Z.; Uhlík, F.; Suzuki, M.; Maeda, Y.; et al. Adamantylidene addition to $M_3N$@$I_h$-$C_{80}$ (M = Sc, Lu) and $Sc_3N$@$D_{5h}$-$C_{80}$: Synthesis and crystallographic characterization of the [5,6]-open and [6,6]-open adducts. *Chem. Eur. J.* **2017**, *23*, 6552–6561. [CrossRef] [PubMed]
55. Sato, K.; Kako, M.; Mizorogi, N.; Tsuchiya, T.; Akasaka, T.; Nagase, S. Bis-silylation of $Lu_3N$@$I_h$-$C_{80}$: Considerable variation in the electronic structures. *Org. Lett.* **2012**, *14*, 5908–5911. [CrossRef] [PubMed]

56. Kako, M.; Miyabe, M.; Sato, K.; Suzuki, M.; Mizorogi, N.; Wang, W.-W.; Yamada, M.; Maeda, Y.; Olmstead, M.M.; Balch, A.L.; et al. Preparation, structural determination, and characterization of electronic properties of bis-silylated and bis-germylated $Lu_3N@I_h$-$C_{80}$. *Chem. Eur. J.* **2015**, *21*, 16411–16420. [CrossRef] [PubMed]
57. Kako, M.; Sugiura, T.; Akasaka, T. Photochemical addition of silirane to endohedral metallofullerene: Electronic properties of carbosilylated $Sc_3N@I_h$-$C_{80}$. *Phosphorus Sulfur Silicon Relat. Elem.* **2016**, *191*, 201–206. [CrossRef]
58. Maeda, Y.; Kimura, M.; Ueda, C.; Yamada, M.; Kikuchi, T.; Suzuki, M.; Wang, W.; Mizorogi, N.; Karousis, N.; Tagmatarchis, N.; et al. Isolation and characterization of [5,6]-pyrrolidino-$Sc_3N@I_h$-$C_{80}$ diastereomers. *Chem. Commun.* **2014**, *50*, 12552–12555. [CrossRef] [PubMed]
59. Cai, T.; Slebodnick, C.; Xu, L.; Harich, K.; Glass, T.E.; Chancellor, C.; Fettinger, J.C.; Olmstead, M.M.; Balch, A.L.; Gibson, H.W.; et al. A pirouette on a metallofullerene sphere: Interconversion of isomers of *N*-tritylpyrrolidino $I_h$ $Sc_3N@C_{80}$. *J. Am. Chem. Soc.* **2006**, *128*, 6486–6492. [CrossRef] [PubMed]
60. Chen, N.; Pinzón, J.R.; Echegoyen, L. Influence of the encapsulated clusters on the electrochemical behaviour of endohedral fullerene derivatives: Comparative study of N-tritylpyrrolidino derivatives of $Sc_3N@I_h$-$C_{80}$ and $Lu_3N@I_h$-$C_{80}$. *ChemPhysChem* **2011**, *12*, 1422–1425. [CrossRef] [PubMed]
61. Li, F.F.; Pinzón, J.R.; Mercado, B.Q.; Olmstead, M.M.; Balch, A.L.; Echegoyen, L. [2 + 2] Cycloaddition reaction to $Sc_3N@I_h$-$C_{80}$. The formation of very stable [5,6]-and [6,6]-adducts. *J. Am. Chem. Soc.* **2011**, *133*, 1563–1571. [CrossRef] [PubMed]
62. Yamada, M.; Mizorogi, N.; Tsuchiya, T.; Akasaka, T.; Nagase, S. Synthesis and characterization of the $D_{5h}$ isomer of the endohedral dimetallofullerene $Ce_2@C_{80}$: Two-dimensional circulation of encapsulated metal atoms inside a fullerene cage. *Chem. Eur. J.* **2009**, *15*, 9486–9493. [CrossRef] [PubMed]
63. Akasaka, T.; Nagase, S.; Kobayashi, K.; Wälchli, M.; Yamamoto, K.; Funasaka, H.; Kako, M.; Hoshino, T.; Erata, T. First evidence for circular motion of metal atoms in endohedral dimetallofullerenes. *Angew. Chem. Int. Ed. Engl.* **1997**, *36*, 1643–1645. [CrossRef]
64. Feng, L.; Suzuki, M.; Mizorogi, N.; Lu, X.; Yamada, M.; Akasaka, T.; Nagase, S. Mapping the metal positions inside spherical $C_{80}$ Cages: Crystallographic and theoretical studies of $Ce_2@D_{5h}$-$C_{80}$ and $Ce_2@I_h$-$C_{80}$. *Chem. Eur. J.* **2013**, *19*, 988–993. [CrossRef] [PubMed]
65. Suzuki, M.; Mizorogi, N.; Yang, T.; Uhlík, F.; Slanina, Z.; Zhao, X.; Yamada, M.; Maeda, Y.; Hasegawa, T.; Nagase, S.; et al. $La_2@C_s$(17490)-$C_{76}$: A new non-IPR dimetallic metallofullerene featuring unexpectedly weak metal–pentalene interactions. *Chem. Eur. J.* **2013**, *19*, 17125–17130. [CrossRef] [PubMed]
66. Kobayashi, K.; Nagase, S.; Maeda, Y.; Wakahara, T.; Akasaka, T. $La_2@C_{80}$: Is the circular motion of two La atoms controllable by exohedral addition? *Chem. Phys. Lett.* **2003**, *374*, 562–566. [CrossRef]
67. Miller, R.D.; Michil, J. Polysilane high polymers. *Chem. Rev.* **1989**, *89*, 1359–1410. [CrossRef]
68. West, R. Polysilanes. In *The Chemistry of Organosilicon Compounds*; Patai, S., Rappoport, Z., Eds.; Wiley: Chichester, UK, 1989; Part 2, Chapter 19, pp. 1207–1240.
69. Fujino, M. Photoconductivity in organopolysilanes. *Chem. Phys. Lett.* **1987**, *136*, 451–453. [CrossRef]
70. Wang, Y.; West, R.; Yuan, C.-H. Fullerene-doped polysilane photoconductor. *J. Am. Chem. Soc.* **1993**, *115*, 3844–3855. [CrossRef]
71. Kepler, R.G.; Cahill, P.A. Photoinduced charge transfer and charge carrier generation in polysilane films containing $C_{60}$ molecules. *Appl. Phys. Lett.* **1933**, *63*, 1552–1554. [CrossRef]
72. Brynda, E.; Nešpůrek, S.; Schnabel, W. Photoconductivity of doped poly(methylphenylsilane). *Chem. Phys.* **1993**, *175*, 459–465. [CrossRef]
73. Watanabe, A.; Tsutsumi, Y.; Matsuda, M. Effect of Si-skeleton dimensionality on optical and electrical properties of poly(methylpenylsilylene) and poly(phenylsilyne). *Synth. Met.* **1995**, *74*, 191–196. [CrossRef]
74. Seki, S.; Shibata, H.; Yoshida, Y.; Ishigure, K.; Tagawa, S. Radiation effects on hole drift mobility in polysilanes. *Radiat. Phys. Chem.* **1997**, *49*, 389–393. [CrossRef]
75. Furukawa, K.; Ebata, K. Preparation and single molecule structure of electroactive polysilane end-grafted on a crystalline silicon surface. *Appl. Phys. Lett.* **2000**, *77*, 4289–4291. [CrossRef]
76. Nešpůrek, S.; Herden, V.; Kunst, M.; Schnabel, W. Microwave photoconductivity and polaron formation in poly[methyl(phenyl)silylene]. *Synth. Met.* **2000**, *109*, 309–313. [CrossRef]

77. Grozema, F.C.; Siebbeles, L.D.A.; Warman, J.M.; Seki, S.; Tagawa, S.; Scherf, U. Hole conduction along molecular wires: σ-bonded silicon versus π-bond-conjugated carbon. *Adv. Mater.* **2002**, *14*, 228–231. [CrossRef]
78. Seki, S.; Koizumi, Y.; Kawaguchi, T.; Habara, H.; Tagawa, S. Dynamics of positive charge carriers on Si chains of polysilanes. *J. Am. Chem. Soc.* **2004**, *126*, 3521–3528. [CrossRef] [PubMed]
79. Seki, S.; Sakurai, Y.; Maeda, K.; Kunimi, Y.; Tagawa, S. Negative resist material based on polysilanes for electron beam and X-Ray lithographies. *Jpn. J. Appl. Phys.* **2000**, *39*, 4225–4230. [CrossRef]
80. Suzuki, H.; Hoshino, S.; Furukawa, K.; Ebata, K.; Yuan, C.-H.; Bleyl, I. Polysilane light-emitting diodes. *Polym. Adv. Technol.* **2000**, *11*, 460–467. [CrossRef]
81. Watanabe, A.; Ito, O. Photoinduced electron transfer between $C_{60}$ and polysilane studied by laser flash photolysis in the near-IR region. *J. Phys. Chem.* **1994**, *98*, 7736–7740. [CrossRef]
82. Acharya, A.; Seki, S.; Saeki, A.; Koizumi, Y.; Tagawa, S. Study of transport properties in fullerene-doped polysilane films using flash photolysis time-resolved microwave technique. *Chem. Phys. Lett.* **2005**, *404*, 356–360. [CrossRef]
83. Watanabe, A.; Ito, O.; Mochida, K. Photoinduced electron transfer from polygermane to $C_{60}$ studied by laser flash photolysis. *Organometallics* **1995**, *14*, 4281–4285. [CrossRef]
84. Lee, J.; Seoul, C.; Park, J.; Youk, J. Fullerene/poly(methylphenylsilane) (PMPS) organic photovoltaic cells. *Synth. Met.* **2004**, *145*, 11–14. [CrossRef]
85. Rybak, A.; Jung, J.; Ciesielski, W.; Ulanski, J. Photovoltaic effect in novel polysilane with phenothiazine rings and its blends with fullerene. *Mater. Sci. Poland* **2006**, *24*, 527–534.
86. Yoshida, K.; Oku, T.; Suzuki, A.; Akiyama, T.; Tokumitsu, K.; Nakamura, M.; Yamada, M. Fabrication and characterization of polysilane: PCBM bulk heterojunction solar cells. *Cent. Eur. J. Eng.* **2013**, *3*, 165–169. [CrossRef]
87. Oku, T.; Nakagawa, J.; Iwase, M.; Kawashima, A.; Yoshida, K.; Suzuki, A.; Akiyama, T.; Tokumitsu, K.; Yamada, M.; Nakamura, M. Microstructures and photovoltaic properties of polysilane-based solar cells. *Jpn. J. Appl. Phys.* **2013**, *52*, 04CR07. [CrossRef]
88. Wakahara, T.; Kondo, T.; Okamura, M.; Akasaka, T.; Hamada, Y.; Suzuki, T.; Kako, M.; Nakadaira, Y. Photochemical bis-silylation of $C_{60}$: Synthesis of a novel $C_{60}$ main chain polysilane. *J. Organomet. Chem.* **2000**, *611*, 78–84. [CrossRef]
89. Wakahara, T.; Kobayashi, J.; Yamada, M.; Maeda, Y.; Tsuchiya, T.; Okamura, M.; Akasaka, T.; Wälchli, M.; Kobayashi, K.; Nagase, S.; et al. Characterization of Ce@$C_{82}$ and its anion. *J. Am. Chem. Soc.* **2004**, *126*, 4883–4887. [CrossRef] [PubMed]
90. Akasaka, T.; Okubo, S.; Kondo, M.; Maeda, Y.; Wakahara, T.; Kato, T.; Suzuki, T.; Yamamoto, K.; Kobayashi, K.; Nagase, S. Isolation and characterization of two Pr@$C_{82}$ isomers. *Chem. Phys. Lett.* **2000**, *319*, 153–156. [CrossRef]
91. Akasaka, T.; Nagase, S.; Kobayashi, K.; Suzuki, T.; Kato, T.; Yamamoto, K.; Funasaka, H.; Takahashi, T. Exohedral derivatization of an endohedral metallofullerene Gd@$C_{82}$. *J. Chem. Soc. Chem. Commun.* **1995**, 1343–1344. [CrossRef]